Wave-equation Migration from Topography

Jeff Shragge and Paul Sava, Stanford University*

SUMMARY

Conformal mapping is a technique used widely in applied physics and engineering fields to facilitate numerical solution of boundary value problems involving solution domains characterized by complex geometry. The predominant reason for applying a conformal mapping procedure is to transform an irregular solution domain to one of symmetric geometry. The conformal map transform has the property that the angle between neighboring arc segments is (locally) conserved under the mapping. Accordingly, in the context of wave-equation imaging under topography, conformal mapping can transform an irregular, topographically-influenced solution domain to a regular computational mesh. In this paper, we demonstrate that the use of the conformal mapping transform coupled with Riemannian wavefield extrapolation generates an orthogonal coordinate system and the governing wavefield continuation equation required for wave-equation migration directly from a topographic surface. We illustrate the potential of this approach by migrating a 2-D prestack data set acquired on a geologic model of thrust belt.

INTRODUCTION

Migration of seismic land data acquired on topography presents a significant imaging challenge. One technique used to correct for the deleterious effects of topography in a more accurate fashion than simple statics corrections is to include a wavefield datuming step in the processing flow (Berryhill, 1979). Usually, this step propagates wavefields down to a common subsurface depth level. However, the presence of strong lateral velocity contrast directly beneath the surface can generate significant wavefield triplication that leads to non-optimal datuming results, especially if Kirchhoff-based methods are used. Therefore, a migration workflow that includes an upward or downward wavefield continuation processing step should produce better imaging results.

However, in practice wavefield continuation is seldom applied directly to data sets acquired on topography without significant pre-processing. The predominant challenge is that the metric of source and geophone arrays seldom conform to a regular computational mesh. Rather, due to instrument cabling, geophone arrays are more likely to uniformly sample the topographic surface. Two common solutions to this problem are either to employ a migration procedure involving wavefield injection (Jiao et al., 2004), or to perform an upward-datuming prior to migration (Bevc, 1997). Migration by wavefield injection commences at the global topographic maximum where the data recorded at this station are injected into the wavefield. The wavefield is then continued downward and data are injected into the wavefield whenever the extrapolation step reaches the height of the topography. Two drawbacks of this approach are that data need to be regularized beforehand to a uniform grid usually through interpolation, and that the additional number of fine-scale extrapolation steps significantly increase cost. Upward wavefield datuming or "flooding the topography" procedures are employed to generate a regular wavefield above the highest point. This processing step can be done successfully with Kirchhoff or other migration operators. One downside of this approach is, again, the increased preprocessing cost. In general, although these methods produce good results, a significant amount of data preprocessing is required to render Cartesian-based wave-equation migration approaches applicable and data fidelity may be compromised.

In this paper, we argue that many of the difficulties with state-of-the-art migration from topography technology could be precluded by abandoning the Cartesian coordinate system for one confor-mal with the topographic surface. To find such a method, we observe that wave-equation imaging is a specific example of a boundary value problem (BVP) that has a solution domain defined by a polygonal boundary. (Images are the superposition of the monochromatic solutions to a number of BVPs of different frequency.) This observation motivates us to examine the results of other applied fields that routinely solve BVPs.

One method routinely employed to help solve BVPs is conformal mapping. This procedure defines how to transform the physical solution domain to a more symmetric canonical domain through mapping in the complex plane (Kythe, 1998). Relating this concept to wave-equation imaging from topography, we suggest using conformal mapping to transform the topographically-influenced physical domain to a canonical domain characterized by a rectangular computational grid. We term this new orthogonal calculation mesh a "topographic" coordinate system. Moreover, the forward and inverse conformal map transforms are also used in defining the wavefield extrapolation equations appropriate for the canonical domain. Consequently, we are both able to perform wavefield extrapolation and to apply the imaging condition in the topographic coordinate domain. The final image is generated by mapping the topographic coordinate image to the physical domain using the inverse conformal mapping transform.

We begin the paper with an overview of conformal mapping illustrated by some simple examples. We then review Riemannian wavefield extrapolation (Sava and Fomel, 2004) and the steps required to generate appropriate wavefield extrapolation equations. The paper concludes with prestack migration results are presented for a data set acquired over a 2-D geological model characterized by severe elevation relief, strong near-surface velocity contrast, and complicated folding and faulting.

CONFORMAL MAPPING

Conformal mapping is a topic of wide-spread interest in the field of applied complex analysis. Generally, this subject deals with the manner in which point sets are mapped between two different analytic domains in the complex plane. In this paper, we refer only to domains that are simply (i.e. not multiply) connected. A mapping between complex planes may be thought of as a rule relating how a field of points defined on a domain in the z-plane, $z = x + iy$, maps to the w-plane, $w = u(x,y) + iv(x,y)$, according to a mapping function, $w = f(z)$ (see the example in Figure 1). If for each point in the z-plane domain there corresponds a unique number in the w-plane, then the mapping function is analytic. In addition, if for each point in the w-plane there corresponds precisely one point in the z-plane, then the mapping is one-to-one and the transformation is invertible. The Cauchy-Riemann equations (Nehari, 1975) are the necessary and sufficient conditions for function $f(z)$ to be analytic in a domain of interest.

A conformal map is distinguishable from other mappings between complex planes by characteristic properties. Most important to this discussion is the conservation of angle property: A conformal mapping of two continuous arcs that locally form an angle α_0 in the z-plane will generate two continuous arcs separated by the same local angle α_0 in the w-plane. Figure 1 illustrates the property that grid lines orthogonal in the w-plane are orthogonal in the z-plane under a conformal map. By extension, non-Cartesian orthogonal coordinate systems can be created in the z-plane (or conversely in the w-plane) by a conformal mapping of a rectangular coordinate system in the w-plane (z-plane). The first major developments in the theory of conformal mapping originated with the mapping theorem

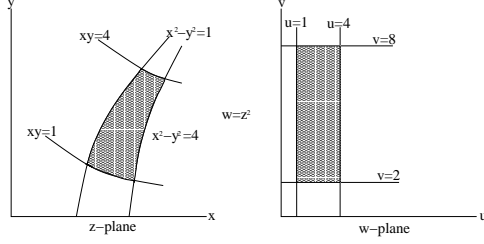**Wave-equation Migration from Topography**

Figure 1: An example of a conformal mapping between the z-plane, $z = x + iy$, and the w-plane, $w(z) = u(x,y) + iv(x,y)$, according to mapping function $w = z^2$. The shaded region in the z-plane maps to the shaded region in the w-plane. Coordinates (u,v) are given by $(x^2 - y^2, 2xy)$. Lines in the w-plane: $u = 1$, $u = 4$, $v = 2$, and $v = 8$, map to the following lines in the z-plane: $x^2 - y^2 = 1$, $x^2 - y^2 = 4$, $xy = 1$. The orthogonality of line intersections in the w-plane are preserved in the z-plane.

of Riemann, who proved the existence of a unique analytic mapping between any two simply-connected, analytic domains. Briefly, let D be a simply-connected region. Then there exists a bijective conformal map $f : D \rightarrow U$, where U is the open unit disk. By extension, if G is a another simply-connected domain, there exists a mapping $g : G \rightarrow U$. Hence, there exists a composite mapping operation, $f \cdot g^{-1} : D \rightarrow G$, between two arbitrary simply-connected domains. Figure 2 illustrates the Riemann mapping theorem between three domains pertinent to the current discussion.
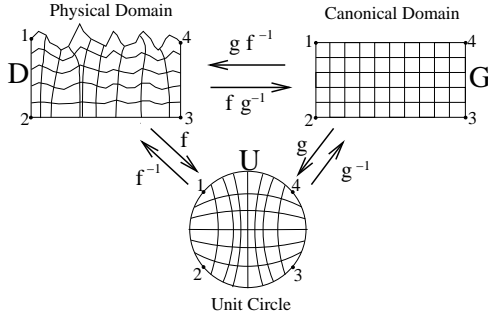

Figure 2: Illustration of the Riemann Mapping Theorem between a physical domain with an undulating upper surface, the unit circle, and a rectangular canonical domain. In this example, a forward mapping function, f, exists between the physical domain and the unit circle and, because the mapping is one-to-one, an inverse mapping f^{-1} also exists. Forward and inverse mapping functions (g and g^{-1}) also exist between the rectilinear domain and the unit circle. Hence, the composition of functions $f \cdot g^{-1}$ denotes a mapping between the physical and canonical domains, while the inverse mapping is given by $g \cdot f^{-1}$. The mapping locations of points labeled 1 through 4 are specified to ensure that the sides in the physical domain correspond to the sides in the canonical domain.

We use the Riemann mapping theorem to transform the topographic domain to a rectangular computational mesh. Assisting us is an extensive catalog of conformal maps between common geometrical domains. Pertinent to the current discussion are the conformal maps between the unit circle (U) and the upper half plane (UHP), $f : U \rightarrow UHP$ and its inverse $f^{-1} : U \leftarrow UHP$,

$$f : z \rightarrow \frac{z - i}{z + i} \quad \text{and} \quad f^{-1} : i \frac{1 + z}{1 - z} \leftarrow z, \qquad (1)$$

and the mapping between the UHP and a rectangle of arbitrary length sides, $g : UHP \rightarrow Rect$, and its inverse $g^{-1} : UHP \leftarrow Rect$,

$$g : w(k) = \int_0^z \frac{d\zeta}{\sqrt{1 - \zeta^2}\sqrt{1 - k^2\zeta^2}} \quad \text{and} \quad g^{-1} : sn(w; k), \quad (2)$$

where g is an elliptic integral of the first kind, k is a function of the ratio of the length of the two sides, and $sn(w; k)$ is a Jacobian elliptic function (Nehari, 1975).

The first step is to define the enclosure of the physical domain where the topographic surface defines the upper boundary. We create the lower boundary by mirroring the topography at twice the maximum extrapolation depth. The side boundaries are defined by straight lines that join the top and bottom segments. The four corner points of the physical domain are also specified. The next two steps involve calculating the forward and inverse mapping functions, f and f^{-1}, between the topographic surface and the unit circle. The fourth step is to generate a rectilinear boundary and to define its four corner points. The next two steps involve calculating forward and inverse mappings functions, g and g^{-1}, between the boundary of the rectangle and the unit circle.

To discern where in the canonical domain to form the coordinate system grid, we need to find the mapping of the topography boundary points on the rectangular domain boundary. This is accomplished by calculating the image of the boundary points under composite mapping operations, $g^{-1} \cdot f$. A rectangular grid is then set up at the image points to create the computational grid. The final step is to map the rectilinear coordinate system, from the canonical domain back to the topographic coordinates under composite mapping operation, $f^{-1} \cdot g$. The resulting point set, z_{topo}^{cs}, defines a coordinate system appropriate for performing wavefield continuation directly from topography at the acquisition locations.

RIEMANNIAN WAVEFIELD EXTRAPOLATION

Performing wavefield extrapolation on topographic computational meshes computed through conformal mapping requires parameterizing the acoustic wave-equation by a set of variables that describe the coordinate system. In 2-D, we denote these variables the extrapolation direction, τ, (analogous to depth in Cartesian wavefield extrapolation), and the direction orthogonal, γ (analogous to horizontal offset in Cartesian wavefield extrapolation). Variables τ and γ are related to the topographic coordinate system point set through $(\tau, \gamma) = (\Re(z_{topo}^{cs}), \Im(z_{topo}^{cs}))$.

The 2-D acoustic wave-equation for wavefield, $\mathcal{U}$, at frequency, ω, governing propagation in topographic coordinates is (Sava and Fomel, 2004),

$$\frac{1}{\alpha J}\left[\frac{\partial}{\partial \tau}\left(\frac{J}{\alpha}\frac{\partial \mathcal{U}}{\partial \tau}\right) + \frac{\partial}{\partial \gamma}\left(\frac{\alpha}{J}\frac{\partial \mathcal{U}}{\partial \gamma}\right)\right] = -\omega^2 s^2 \mathcal{U}, \qquad (3)$$

where s is the slowness of the medium, α a distance scaling factor in the extrapolation direction τ, and J a Jacobian of transformation of coordinate γ (analogous to a geometrical ray spreading factor). Parameters α and J are defined by

$$\alpha = \left[\frac{\partial x}{\partial \tau}\frac{\partial x}{\partial \tau} + \frac{\partial z}{\partial \tau}\frac{\partial z}{\partial \tau}\right]^{\frac{1}{2}} \quad \text{and} \quad J = \left[\frac{\partial x}{\partial \gamma}\frac{\partial x}{\partial \gamma} + \frac{\partial z}{\partial \gamma}\frac{\partial z}{\partial \gamma}\right]^{\frac{1}{2}} \quad (4)$$

where x and z are the coordinates of the underlying Cartesian basis. Note that parameters α and J are solely components of the coordinate system and are independent of the extrapolated wavefield values.

Analogous to wavefield continuation on a Cartesian mesh, a dispersion relation must be specified that forms the basis for all derived extrapolation operators in a topographic coordinate system.

Wave-equation Migration from Topography

The relation being sought is the wavenumber along the extrapolation direction, k_τ. Following Sava and Fomel (2004), the partial derivative operators in (3) are expanded out to generate a second-order partial differential equation with non-zero cross derivatives. Fourier-domain wavenumbers are then substituted for the partial differential operators acting on wavefield, $\mathcal{U}$, and the quadratic formula is applied to yield the expression for k_τ,

$$k_\tau = \frac{i\alpha}{2J}\frac{\partial}{\partial\tau}\left(\frac{J}{\alpha}\right) \pm \tag{5}$$

$$\left[(\omega s\alpha)^2 - \left(\frac{\alpha}{2J}\frac{\partial}{\partial\tau}\left(\frac{J}{\alpha}\right)\right)^2 + \frac{i\alpha}{J}\frac{\partial}{\partial\gamma}\left(\frac{\alpha}{J}\right)k_\gamma - \frac{\alpha^2}{J^2}k_\gamma^2\right]^{\frac{1}{2}}.$$

One relatively straightforward way to apply wavenumber k_τ in an extrapolation scheme is to develop the topographic coordinate system equivalent to a phase-screen extrapolation operator. In the following example, we treat solely the kinematic, one-way propagation of recorded wavefields. This asymptotic approximation leads us to drop the first-order partial differential terms in (5),

$$k_\tau = \pm\sqrt{a^2\omega^2 - b^2 k_\gamma^2}, \tag{6}$$

where $a = s\alpha$ and $b = \alpha/J$. The expansion of k_τ about reference parameters a_0 and b_0 is,

$$k_\tau \approx k_{\tau 0} + \left.\frac{\partial k_\tau}{\partial a}\right|_{a_0,b_0}(a - a_0) + \left.\frac{\partial k_\tau}{\partial b}\right|_{a_0,b_0}(b - b_0), \tag{7}$$

where subscript 0 denotes reference. Partial derivatives with respect to parameters a and b are,

$$\left.\frac{\partial k_\tau}{\partial a}\right|_{a_0,b_0} = \omega\frac{1}{\sqrt{1-\left(\frac{b_0 k_\gamma}{\omega a_0}\right)^2}} \approx \omega\left[1 + \frac{c_1\left(\frac{b_0 k_\gamma}{\omega a_0}\right)^2}{1-3c_2\left(\frac{b_0 k_\gamma}{\omega a_0}\right)^2}\right], \tag{8}$$

$$\left.\frac{\partial k_\tau}{\partial b}\right|_{a_0,b_0} = -\omega\frac{b_0}{a_0}\left(\frac{k_\gamma}{\omega}\right)^2\frac{1}{\sqrt{1-\left(\frac{b_0 k_\gamma}{\omega a_0}\right)^2}} \approx -\omega\frac{b_0}{a_0}\left(\frac{k_\gamma}{\omega}\right)^2,$$

where the square root function in the denominator has been expanded using a Padé approximation. The choice of numerical constants $c_1 = \frac{1}{2}$ and $c_2 = 0$ yields a 15° finite-difference term, and a phase-screen approximation for extrapolation wavenumber, k_τ,

$$k_\tau \approx k_{\tau 0} + \omega(a - a_0) + \omega\frac{\left[c_1\left(\frac{a_0}{b_0}\right)^2(a-a_0) - \frac{b_0}{a_0}(b-b_0)\right]\left(\frac{k_\gamma}{\omega}\right)^2}{1 - 3c_2\left(\frac{b_0}{a_0}\right)^2\left(\frac{k_\gamma}{\omega}\right)^2}. \tag{9}$$

Extending this approach to include multiple reference media (e.g., phase-shift plus interpolation (Gazdag and Sguazzero, 1984)) over the two parameters is possible; however, this extension is not treated here. The approximation for wavenumber, k_τ, given in (9) is used in a conventional wavefield extrapolation scheme that extends the recorded wavefield away from the acquisition surface into the subsurface. This involves solving a one-way wave-equation. Our prestack migration example is computed using a shot profile migration code. This involves extrapolating the source and receiver wavefields, $\mathcal{S}$ and $\mathcal{R}$, independently using,

$$\mathcal{S}_{\tau+\Delta\tau} = \mathcal{S}_\tau e^{-ik_\tau\Delta\tau} \quad \text{and} \quad \mathcal{R}_{\tau+\Delta\tau} = \mathcal{R}_\tau e^{ik_\tau\Delta\tau} \tag{10}$$

and applying an imaging condition to generate image, $\mathcal{I}(\tau,\gamma)$,

$$\mathcal{I}(\tau,\gamma) = \sum_i\sum_w \mathcal{S}(\tau,\gamma,\omega;\mathbf{s_i})\overline{\mathcal{R}(\tau,\gamma,\omega;\mathbf{s_i})}, \tag{11}$$

where the line over the receiver wavefield indicates complex conjugate. Image $\mathcal{I}(\tau,\gamma)$ is then mapped to a Cartesian coordinate system using sinc-based interpolation operators in the neighborhood of each mapped point to generate the final image, $\mathcal{I}(x,z)$.

NUMERICAL EXAMPLES

We test the conformal mapping and Riemannian wavefield extrapolation approach on a synthetic dataset computed on a rugged topographic surface. The geological model is a merger of common geologic features from the Canadian Foothills. The velocity model, shown in the top panel of Figure 4, consists of steep thrust fault planes and complex folds typical of a mountainous thrust region. The topographic boundary of interest is demarcated by the velocity model discontinuity nearest to the surface. The total relief of the Earth's surface in this model is 1600 m. Also note that the complex near-surface velocity structure should present a significant imaging challenge (Gray and Marfurt, 1995).

Figure 3 shows the a conformally mapped coordinate system that incorporates the topography shown in top panel of Figure 4. One important observation is that topography causes focusing of the coordinate system. In particular, the coordinate system compresses under local topographic maxima, and expands beneath local topographic minima. This suggests that Jacobian spreading factor J in (3) will be strongly dependent on the local radius of curvature of the topographic surface. However, as the topographic fronts move farther from the surface, the topographic influenced diminishes and the fronts move toward becoming a flat datum. (Hence, this approach could also be used for wavefield datuming.)
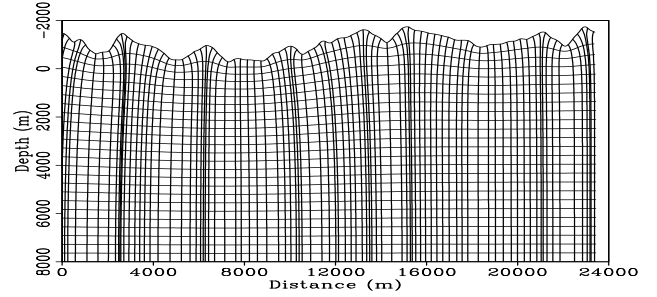

Figure 3: Conformally mapped topographic coordinate system. Note the compression (extension) of the rays under topographic maxima (minima). The influence of topography on the coordinate system diminishes farther from the surface.

A prestack wave-equation imaging test was conducted using a synthetic data set generated by an acoustic, 2-D, finite-difference code. The data set is comprised of 278 shot gathers with a split-spread geophone geometry where absolute offsets range between 15 m and 3600 m. Geophone and source spacing are 15 m and 90 m, respectively. Data were generated on a regular Cartesian mesh. Thus, we interpolated the data to fit on a grid uniform along the topographic surface. Data fidelity may have been lowered by this processing step; however, we emphasize that this step is normally of modest importance since field data likely are nearly uniformly spaced on the topographic surface.

A preliminary prestack migration image is presented in Figure 4. The majority of reflectors are well positioned; however, diffractions and discontinuous reflectors exist at locations directly beneath topographic minima and maxima. Although these anomalies may be caused by the data regularization procedure, they more likely arise from limitations imposed by the phase-screen approximation. Also present are vertical streaks of higher (lower) amplitude directly under local topographic minima (maxima). We
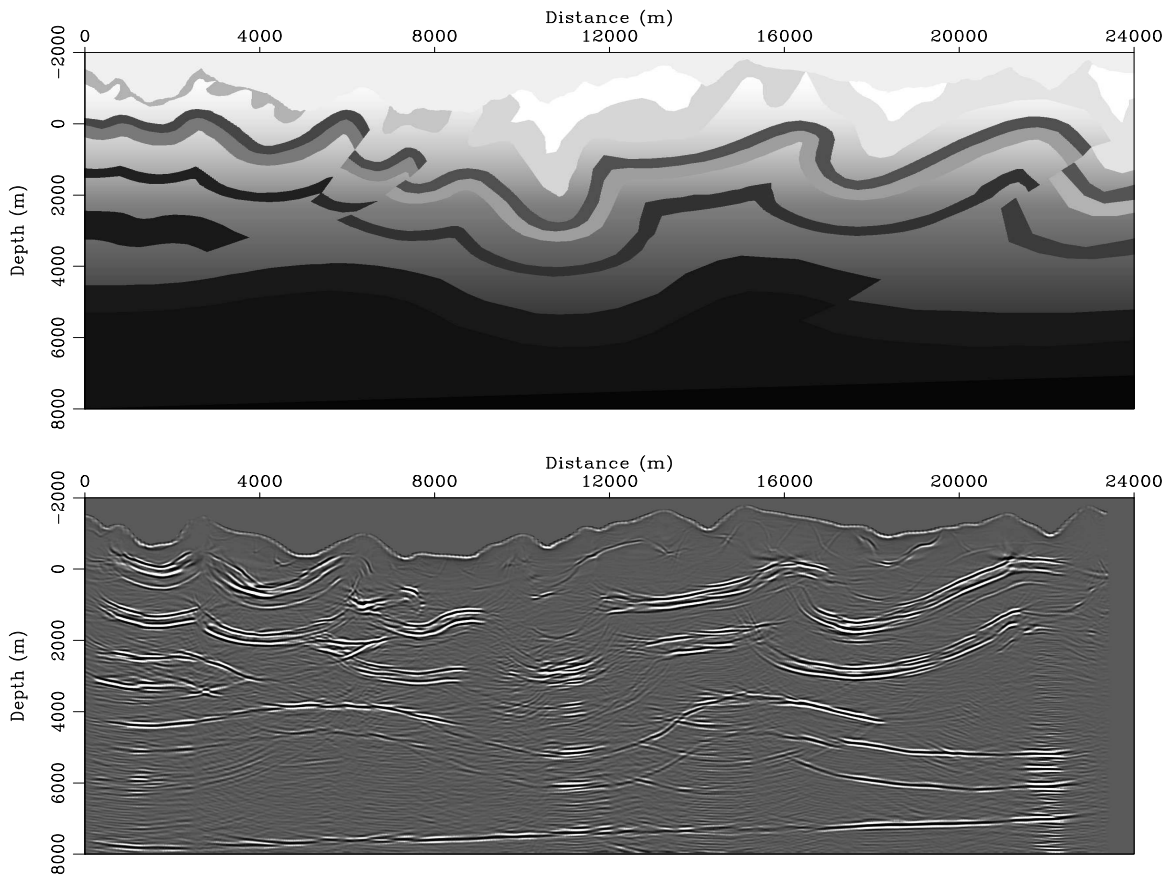
Wave-equation Migration from Topography

Figure 4: Top: Canadian Foothills velocity model constructed from composite 2-D geologic model. Total elevation relief is approximately 1600 m. The topographic boundary of interest is demarcated by the velocity model discontinuity nearest to the surface. Bottom: The preliminary prestack migration image using Riemannian wavefield extrapolation on a coordinate system generated through conformal mapping.

attribute these anomalous amplitudes to a combination of: i) the simplicity of the weighing function used in the interpolation of the image between the topographic and Cartesian coordinate systems; and ii) our non-consideration of the dynamic terms in (6). Geological structure poorly imaged or absent include sections of the steeply-dipping fold belt, which is probably due to limitations imposed by both the limited angular bandwidth of the phase-screen approximation, and our use of only one reference medium.

CONCLUDING REMARKS

Performing wave-equation migration directly from topographic surfaces is achievable with a minimum of preprocessing in topographic coordinate systems. We show that conformal mapping generates the required topographic coordinate systems, and that the conformal map transform determines the appropriate wavefield extrapolation equations. We also conclude that multiple reference media are likely needed to image under complicated topography, which is consistent with wavefield extrapolation practice in a Cartesian coordinate system. By extension, we show that upward datuming on a coordinate system generated through conformal mapping transformation could work as a pre-imaging processing step. Moreover, upward datuming could be more effective than downward migration direct from topography, since a constant velocity function would likely improve the range over which the phase-screen approximation is accurate. Standard Cartesian-based migration technology could then be used to downward continue the upward datumed wavefields.

REFERENCES

Berryhill, J., 1979, Wave-equation datuming: Geophysics, **44**, 1329–1344.

Bevc, D., 1997, Floodint the topography: Wave-equation datuming of land data with rugged acquisition topography: Geophysics, **62**, 1558–1569.

Gazdag, J., and Sguazzero, P., 1984, Migration of seismic data by phase-shift plus interpolation: Geophysics, **69**, 124–131.

Gray, S., and Marfurt, K., 1995, Migration from topography: Improving the near-surface image: J. Can. Soc. Expl. Geophys., **31**, 18–24.

Jiao, J., Trickett, S., and Link, B., 2004, Wave-equation migration of land data: 2004 CSEG Convention, CSEG, CSEG Abstracts.

Kythe, P., 1998, Computational conformal mapping: Birkhäuser, Boston, MA.

Nehari, Z., 1975, Conformal mapping: Dover Publications Inc., New York.

Sava, P., and Fomel, S., 2004, Seismic imaging using Riemannian wavefield extrapolation: submitted to Geophysics.